

SOLUTION MINING RESEARCH INSTITUTE

812 MURIEL STREET
WOODSTOCK, ILLINOIS 60098
815-338-8579

MEETING
PAPER



A METHODOLOGY FOR COMPARING INTERNAL CEMENT MORTAR LININGS FOR CORROSION PROTECTION OF BRINE PIPELINES WITHIN THE STRATEGIC PETROLEUM RESERVE*

T. E. Hinkebein

Underground Storage Technology Department 6113
Sandia National Laboratories
Albuquerque, NM 87185-0706

R. G. Buchheit, L. M. Maestas

Mechanical and Corrosion Metallurgy Department 1832
Sandia National Laboratories
Albuquerque, NM 871850340

**Solution Mining Research Institute Spring Meeting
New Orleans, Louisiana
May 2, 1995**

ABSTRACT

Internal cement mortar linings for brine pipelines in the Strategic Petroleum Reserve (SPR) were tested for corrosion protection using a combination of laboratory and field experimental procedures. Samples of lined pipe were exposed to the corrosive brine environment at the Big Hill SPR facility and in the laboratory. Specimens were returned to the lab where several tests were performed. Visual observation of the interfacial area provided the an initial determination of the performance of the lining materials. Electron probe microanalysis (EPMA) determined the chemical analysis of the damaging species, such as Cl, in cement-mortar linings. Interfacial shear strength measurements provided a measurement of the cement-steel bond condition. Electrochemical impedance spectroscopy (EIS) provided a measure of the **charge** transfer resistance associated with the passive area as well as the apparent corrosion rate.

* This work has been sponsored by the U.S. Department of Energy.

A Methodology for Comparing Internal Cement Mortar Linings for Corrosion Protection of Brine Pipelines within the Strategic Petroleum Reserve

by

T. E. Hinkebein, R. G. Buchheit, L. M. Maestas

INTRODUCTION

The SPR operates approximately 65 miles of **brine** disposal pipelines. Over **the** history of the **SPR**, these pipelines have experienced aggressive corrosion and erosion damage. As a result corrosion mitigating measures are now being pursued to increase the service lifetimes. The most significant of these measures is **the** use of internal cement linings. A number of mortar compositions are being tested to determine the projected benefits associated with the use of these **mortars** as lining materials. Cement linings are being considered because they provide corrosion protection by passivating the steel in the high **pH** environment of cement paste as well as providing erosion protection from insoluble solids which are produced with the brine. A study of these cement lined pipes is presented **which** will allow us to determine not only the performance but to determine a projection of future performance of the pipeline system. In this paper we will describe the materials, the sample preparation techniques, the exposure conditions, the analytical techniques used and some interim results of **the** study.

CEMENT LINING MATERIALS

Five basic classes of cements are being evaluated in this study. These include the following:

1. standard API RP**10E**¹ formulation
2. standard API RP **10E** formulation modified with latex
3. standard API RP **10E** formulation modified with epoxy

4. standard API RP **10E** formulation modified with sodium nitrite
5. calcium-aluminate cement

The API RP **10E** is a blend of 60% high sulfate resistant Portland cement and 40% Class F fly ash. This cement is mixed with a minimum amount of water and **centrifugally** applied in a gravitational field of at least 18g. The resultant lining is extremely dense and provides a good corrosion barrier for common oil field service. However, for the aggressive conditions experienced in brine service, other standards (particularly the German Industrial **Standard**²) indicated that this formulation might be inadequate. Consequently, a number of other cement formulations were investigated. Firstly, the mixture composition of the **10E** composition was varied away from the **60-40** blend of cement and fly ash. Secondly, up to 15% latex was added to the **10E** formulation. Latex is frequently added to the concrete used in parking garages and bridge decking to resist deterioration as a result of road salt. Thirdly, the **10E** formulation was modified with the addition of an inverted emulsion of epoxy. As **with** latex the epoxy formulation has been used in commercial applications to protect cement **from** a high salinity **environment**. The forth variation was the addition of small amounts (2%) of the passivating agent sodium nitrite to the cement. This modification has found success in the laboratory by enhancing the formation of the passive layer at the steel-cement interface. The last cement mixture was a calcium-aluminate cement formulation called out in the German Industrial Standard. This particular formulation has been used in brine pipeline service in the German oil reserve.

SAMPLE PREPARATION

Centrifugally cast test specimens were fabricated using the standard API centrifugal casting **methods**³. In this process cement mortars were prepared in mixing bins, then pumped through a delivery lance into the pipe section to be lined. The pipe section was capped at one end and the mortar was pumped as a predetermined rate as the lance was withdrawn. After charging the pipe section the open end of the pipe was capped and the pipe was loaded onto rollers for the spinning operation. Pipe sections were spun at greater than 18 g for 1.5 to 4 minutes. After spinning the end caps were removed and the excess water was drained from the pipe. The pipe sections were then cured at 150 °F overnight in the case of the API formulations or at ambient conditions for the calcium-aluminate cements.

In addition to the centrifugally cast specimens, several hand troweled specimens were also prepared. These specimens were formulated with the API RP 10E baseline material and the calcium-aluminate cement. Hand troweling is the method used to coat fittings and the resultant lining is not as dense as the centrifugally cast lining. Hand troweled specimens were cured in the same way as were the centrifugally cast samples.

EXPOSURE CONDITIONS

In order to test these specimens in an efficient manner, the following experimental conditions are being used:

1. flow loop test
2. immersion tests
3. lab tests
4. full scale test

The flow loop is a scaled test system constructed at the Big Hill SPR site in Winnie, TX. This test measures the durability of the cement mortar lining and

pipe corrosion rate with actual brine generated from normal site operations. In the flow loop, three-inch diameter cement lined test pipes were placed in a manifold through which brine was pumped at a rate to simulate the wall shear stress of a **36-inch** diameter brine pipeline carrying brine at 830,000 **BBL/day**. Linear polarization probes, fitted into diametrically opposing ports in the pipe prior to the pipe lining operation, were used to measure instantaneous corrosion rates.

The immersion test were conducted in the brine pond at the Big Hill site. In these tests, three-inch diameter pipe samples were allowed to soak in the brine pond for varying time periods. There were twelve samples of each of the material types placed in the brine pond. During the immersion period the samples experienced a relatively static or low flow condition. At periodic intervals sample removals were performed and the samples were returned to Sandia National Laboratories for analysis. The laboratory analyses performed on the returned samples are described below.

To supplement the field testing, laboratory based Electrochemical **Impedance Spectroscopy (EIS)**, described in the next section, was performed in cells constructed from cement-mortar lined pipe sections. These specimens were made from **3-inch** diameter lined pipe and were 4 in. long. They were filled with a **synthetic** brine consisting of 300 g/l **NaCl**, 4.0 g/l **CaSO₄**, and 1.0 g/l **MgCl₂** which approximated saturated SPR brine. Air sparging kept the dissolved oxygen concentration near its saturation value of 2 **ppm**.⁴ The use of saturated brine insured that the composition of the brine remained constant during the lengthy test.

In addition to the testing performed on small sized test specimens, a limited number of full sized field test have been undertaken on a **24-inch** diameter brine header at the West Hackberry SPR facility. This brine header is

being studied as part of a one year program to extend the laboratory and small scale field test results. Corrosion is being investigated in this test using the EIS technique.

DISCUSSION OF ANALYTICAL TECHNIQUES

Visual Observation

The first method used to determine the performance of any particular lining material was visual observation. After samples were returned to the laboratory, the pipe samples were cut in half longitudinally and the cement lining was removed from one of the halves. The exposed pipe was visually inspected for corrosion. While visual observation is a relatively qualitative technique, it does allow for a rank ordering of the performance of the lining materials.

Instantaneous Corrosion Rates

For those samples fitted with linear polarization probes, instantaneous corrosion rate measurements were made using a 10 mV voltage perturbation about the free corrosion potential. Corrosion rates were determined from the polarization resistance using the **Steam-Geary⁵** equation. This method of determining corrosion rates assumes a proportionality factor between the polarization resistance and the corrosion rate. For cement lined steel pipes it was observed **that** the corrosion at the steel-mortar interface was **localized**. Further, the probes used for this determination were relatively small, 1/8 in. in diameter. As a consequence, these probes reported erratic results for the **performance** of the lining material.

Electron Probe Microanalysis (EPMA)

For those samples returned to the laboratory for analysis, electron probe microanalysis (EPMA) was performed to determine the ingress of brine and the degradation of cement liners as a function of exposure time.

Sections of the liner were removed, potted in epoxy and polished with successively finer papers and diamond pastes until the surface **was** sufficiently smooth for X-ray microanalysis. X-ray line scans were performed using a electron microprobe. Analyses were conducted by stepping the beam in **50 μ m** increments from the **steel-mortar** interface. Quantitative wavelength dispersive X-ray data were generated using a 25 nA beam. All of the major elements expected in a **steel-cement-brine** system were measured although the focus for this study has been determined to be the distribution of chlorine (as chloride).

Interfacial Shear Strength Test

In addition to the **EPMA** chemical analyses on samples returned from the brine pond, the steel-mortar interfacial shear strength was measured using a standard push test. In these test the force required to displace the cement mortar liner longitudinally was determined as the force at which the **force-displacement** curve was offset from linearity by 0.002 in. of stroke displacement. Samples for this test were 3 inches in diameter and approximately 1 in. in length. The strength of the steel-cement interface was determined on samples returned from the brine pond so that a time dependent variation was obtained. The bond strength in an important parameter since the expected failure mode for mortar **lined** pipe is the separation of the mortar liner **from** the steel pipe. As corrosion products build up under the liner, it is believed that these more bulky compounds will crack the liner and cause it to separate from the steel.

Electrochemical Impedance Spectroscopy (EIS)

To address the erratic behavior associated with the measurement of instantaneous corrosion rate, electrochemical impedance spectroscopy (**EIS**) was employed to supplement the other studies. EIS is a

technique which can give kinetic and mechanistic information about the corrosion process. To implement this technique a two electrode measurement cell was constructed in the lab. The mortar-lined steel pipe, which formed the working electrode, was sealed on one end with rigid plastic. The pipe was filled with simulated brine and air was continuously bubbled through the solution. A cylindrical nichrome screen formed the counter electrode. A 20 mV sinusoidal voltage perturbation was applied across the electrodes. The resulting complex impedance gives information about the corrosion state of the whole steel-mortar interface, and the diffusional resistance of the cement mortar liner. A complex plane plot representative of the response of mortar lined steel pipe is shown in Figure 1. The inset shows a small arc or 'spur' observed at high frequencies. The low frequency arc was semicircular and depressed with respect to the real axis. The high frequency arc was not always fully resolved, but also appeared to be a depressed semicircle. The time constant for the high frequency arc was typically in the range of 10^{-3} to 10^{-4} s. while the low frequency arc was usually between 300 to 1000 s.

According to Macdonald⁶, the complex impedance is represented by an equivalent electrical circuit. In this model two parallel sub circuits are used to represent corroding and passivated regions of the steel-mortar interface as shown in Figure 2a. These parallel sub circuits are arranged in series with a cement resistance, R_c . The sub circuit for the passivated area of the interface is comprised of a capacitance, C_{pa} , in parallel with a charge transfer resistance, R_{pa} . The sub circuit for the corroding area of the interface is comprised of a capacitance, C , in parallel with a charge transfer resistance, R_{ca} , and a diffusional impedance, Z_w . A_{pa} and A_{ca} in Figure 2a denote the passivated area fraction and the corroding area fraction respectively. Charge transfer processes occurring at passive areas are excited at high frequencies and those

occurring at corroding areas are excited at lower frequencies.

For complex nonlinear least squares fitting of the individual arcs in Figure 1, a more generalized form of the model in Figure 2a was adopted. In the modified equivalent circuit shown in Figure 2b, the low frequency arc was modeled using a resistor in parallel with a constant phase element; a combination otherwise known as a ZARC impedance function⁵. As shown in Figures 3a and 3b, this equivalent circuit was capable of accurately fitting spectra from mortar lined steel pipe. The high frequency arc is not always fully resolved, and fitting is not performed. The Z' intercept of the low-frequency side of the arc was used for estimating R_{pa} .

This generalized model was used to reflect the fact that charge transfer and diffusional impedances were not clearly distinguished in the impedance response of these systems. Use of the ZARC function is appropriate for modeling systems where the relaxation time is not single valued but distributed about some mean value'. In mortars, the conductive pathways are the Portland cement paste, and shrinkage cracks filled with intruding brine. Many of these pathways exist in the liner with similar, though not identical relaxation times. Additionally, this and previous studies⁸ suggest that the mean time constant for diffusional processes in the cement mortar, and the time constant due to charge transfer at a corroding steel-mortar interface are similar. Separating out the diffusional impedance is further complicated by the fact that good mass transport data are not readily available for cements of the type under study here. The ZARC function allows the lumped quantities, R_{pa} and R_{ca} , to be determined without having to distinguish among the diffusion and charge transfer components.

The measured value of the charge transfer resistance associated with the passivated

interface, R_{pa}^m , is related to the passive interfacial area, A_{pa} , by

$$R_{pa}^m = \rho_{pa}^o / A_{pa} \quad (1)$$

where ρ_{pa}^o is the area specific resistivity of the passive interface. This equation demonstrates that the resistance associated with the passive is also related to the area of the **steel-mortar** interface that is not corroding. Additionally, the measured value of the charge transfer resistance associated with the corroding area, R_{ca}^m , is related to the measured corrosion current, I_{corr} , by

$$I_{corr} = B / R_{ca}^m \quad (2)$$

where B is an experimentally determined transfer coefficient. The value of B for actively corroding plain carbon steel in saturated $Ca(OH)_2$ plus mortar additives is 26 mV⁹. The corrosion current is linearly related to the corrosion rate.

TYPICAL SUMMARY OF TESTING RESULTS

Visual Observations

The visual observation of samples returned from the brine pond at Big Hill allowed for the first major discrimination among the tested cement mortar lining materials. From the condition of the steel surface of returned samples, it was determined that some materials were performing significantly better than others. In particular the baseline material, calcium-aluminate cement mortars and the sodium nitrite modified cement mortars showed little evidence of corrosion during the first six months of service. Further, the latex modified and the epoxy modified mortars showed only slightly more evidence of corrosion. The cements with compositional variations away from the baseline API formulation showed larger patches of corroding areas. Hand troweled

sections of the baseline API material showed general corrosion within two months.

EPMA

Figure 4 demonstrates the application of the use of the electron microprobe for the comparative study of the latex modified mortar and the baseline material. Figure 4a is a plot of chloride concentration as a function of position in the 5% latex modified cement mortar liner after 60 days exposure to brine at Big Hill. This plot illustrates how brine is transported and partitioned in the mortar. The main feature of this plot is the high Cl concentration near the mortar-brine interface due to the penetration of brine through the paste. Smaller spikes are the result of shrinkage cracks in the liner that filled with brine during the exposure. These cracks appear to deliver brine to the steel interface where Cl level are elevated. Elevated Cl levels at the steel interface were observed after 30 days exposure to SPR brine.

Figure 4b shows a similar profile of Cl concentration in the baseline material after 60 days. In this case the Cl concentration at the interface is less. Further, secondary spikes resulting from shrinkage cracks are absent in this plot. Thirdly, the position of the maximum in the chlorine front as a function of time is plotted in Figure 5 as a measure of the brine ingress through the paste. The brine is observed to penetrate farther in the case of the latex modified cement than in the baseline case.

Similar results were obtained for the calcium-aluminate mortar. In Figure 6a the depth of penetration of the main peak is presented for the calcium-aluminate **cement**, baseline, and hand-troweled baseline materials. The average concentration within 2 mm. of the steel interface is presented in Figure 6b. Note that the hand-troweled material shows chlorine breakthrough very quickly. The calcium-aluminate mortar is

still providing excellent protection after 3 years.

Inter-facial Shear Strength Test

Some results **from** the shear strength testing of 5% latex modified cement mortar liners and the baseline liners are presented in Figure 7. Both of these liners give approximately similar results although the variability of the results makes comparison difficult. The mean bond strength for the latex modified cement is 240 psi while the mean bond strength of the baseline material is 180 psi. While these strengths are not greatly different they do provide an indication that the bond strengths of these materials is not one of the more important properties in separating the performance of these materials.

Bond strengths are also presented for the baseline, hand troweled, and calcium-aluminate materials in Figure 8. In this case the bond strengths of the hand troweled material deteriorates rapidly after the first month and this performance reflects the corrosion response of the troweled baseline material. The calcium-aluminate bond strengths are much higher than the baseline materials.

EIS Results

Figure 9 shows the measured charge transfer resistance associated with the passivated **interface**, R_{pa}^m , as a function of the exposure time for the baseline and latex modified concretes. Assuming that the area specific resistivity is similar for each type of cement, Equation (1) illustrates the inverse relationship between the charge transfer resistance and the passive interface area. Hence, this figure indicates that the baseline material exhibit a larger passive interfacial area than the latex modified cements for exposure times up to 100 days. After this **time**, R_{pa}^m for the 5% latex cement concrete appears to fall suggesting that corroding area

is passivated. The 10% and 15% latex modified cements exhibit high R_{pa}^m , presumably indicating smaller passive interface areas in the high frequency response.

Figure 10 shows the charge transfer resistance of the corroding areas as a function of **the** exposure time. These data are highly scattered, but during the first 180 days the general trend is that the largest R_{ca} are exhibited by the latex modified cement. Based upon Equation (2) the apparent corrosion rate is larger for the baseline material initially but that this **difference** narrows as time progresses.

Figure 11 shows the high frequency charge transfer resistance, R_{pa}^m , for the calcium-aluminate mortar and the baseline mortar. The general trend for all curves **is that the** passive area is reduced with time. The calcium-aluminate air-cured mortar shows a similar fraction of passive area as the baseline. The low frequency response, R_{ca}^m , for the calcium-aluminate mortars is presented in Figure 12. The air-cured calcium-aluminate mortar demonstrated an order of magnitude lower corrosion rate than the baseline material.

SUMMARY

The techniques of using a combination of electrochemical impedance spectroscopy and electron probe microanalysis (**EPMA**) provide a much more accurate method of discriminating the corrosion protection performance of cement lined pipe than the more traditional method of using linear polarization probes. **The** Primary improvements lie in the ability to interrogate a larger portion of the pipe under the **cement-mortar** lining. The EIS response originates from a partially corroding interface. The high frequency response is related to the passive area while the low frequency response is associated with the corroding area. The trend in the high frequency response is

consistent with a decreasing passive area with increasing exposure time. Further, **EPMA** allows a determination of compositional information which allows a projection of future performance.

Acknowledgement

We wish to thank Paul Hlava and Tom Crenshaw for their assistance with this study. Paul was responsible for **the** operation of the microprobe and interpretation of **the** results. Tom was responsible for the shear **strength** measurements and **their** interpretation.

¹**API RP 10E**, "Recommended Practice for Application of Cement Lining to Steel Tubular Goods, Handling, Installation and Joining, Amer. Pet. Inst., Washington, 1987.

²**DIN 2614**, "Cement Mortar Linings for Cast Iron Pipes, Steel Pipes, and Fittings: Methods Requirements, Tests, Beuth Verlag **GmbH**, Berlin, Feb. 1990.

³**B. Jackson, J. F. Armstrong**, Materials Performance, 29, 2 (**1990**), p. 36.

⁴**Daily Meter Reading Data Sheets**, Big Hill site, Winnie, **TX**, 1990-1991.

⁵**M. Steam, A. L. Geary**, J. Electrochemical Soc., 104 (**1957**), p. 56.

⁶**D. D. Macdonald, M. C. H. McKubre, M. Uruquidi-Macdonald**, Corrosion, 44 1 (**1988**), p. 2.

⁷**J. R. Macdonald, D. R. Franschetti**, "Physical and Electrochemical Models", Impedance Spectroscopy, (New York: John Wiley and Sons, Inc., **1987**), p. 90.

⁸**D. G. John P. C. Searson, J. L. Dawson**, British Corrosion Journal, 16 2 (**1981**), p. 102.

⁹**C. Andrade, J. Gonzales**, Werk. u. Korr., 29 (1978) p. 515-519.

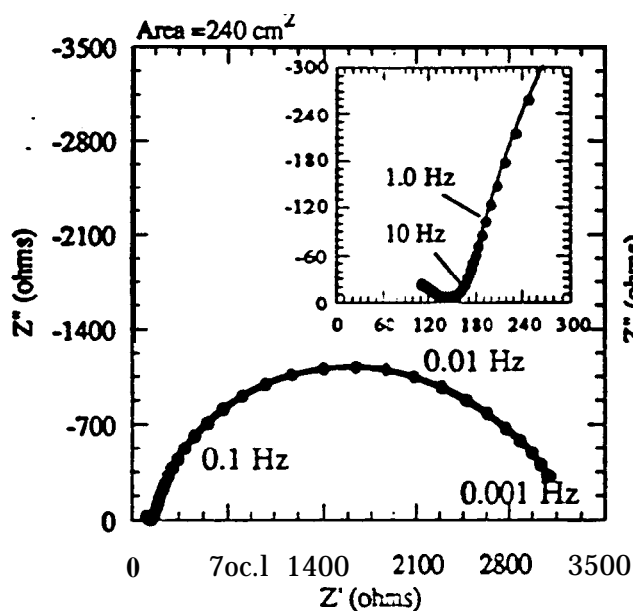


Figure 1. Typical Complex plane plot for the concrete lined steel pipe used in EIS experiments.

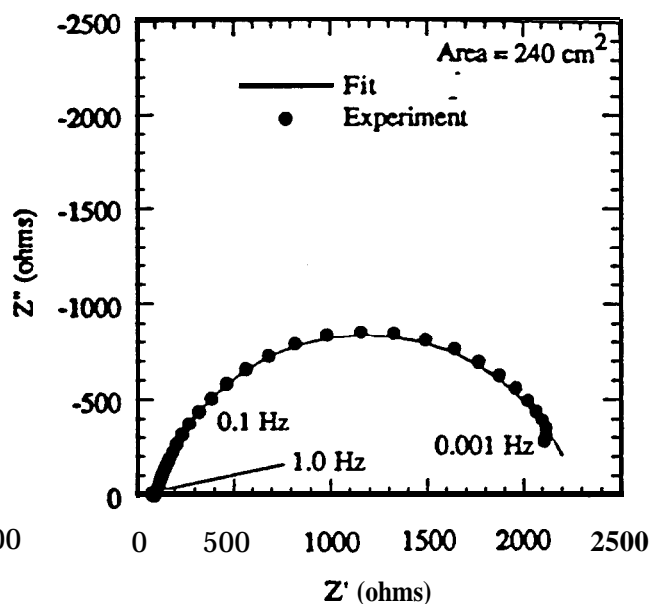


Figure 3a. Experimental EIS data and CNLS fit using the model shown in Figure 2b for the baseline concrete liner.

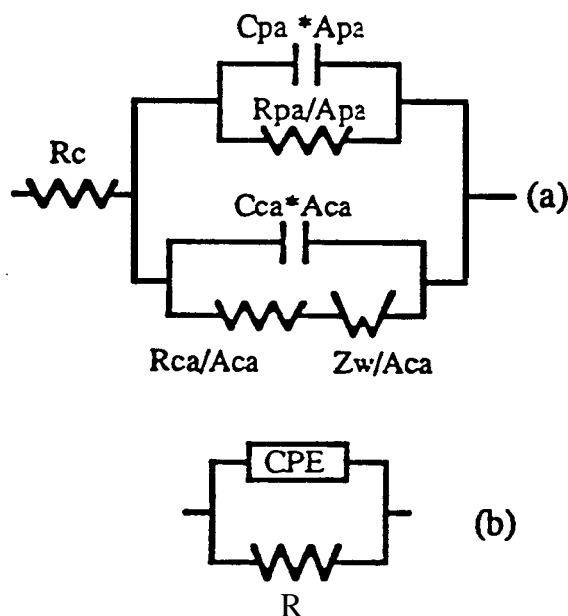


Figure 2. (a) Equivalent circuit used for interpreting EIS data, (b) generalized form used for CNLS modeling of the low frequency arc.

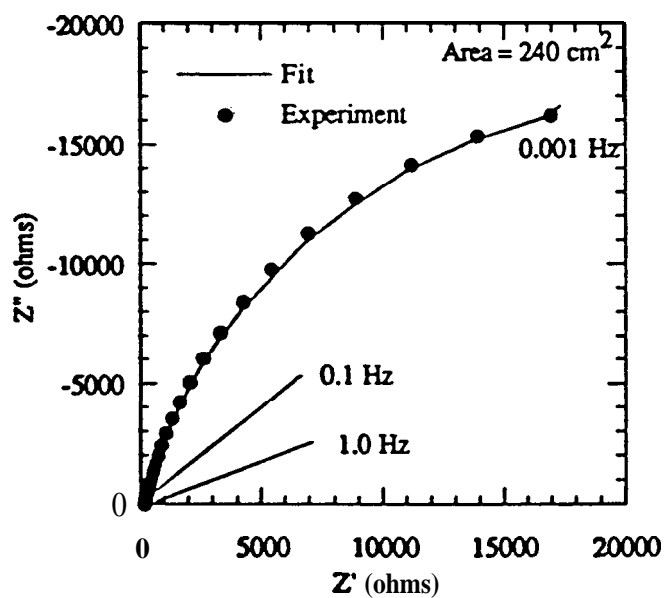


Figure 3b. Experimental EIS data and CNLS fit for 5% latex modified concrete liner after 14 days exposure.

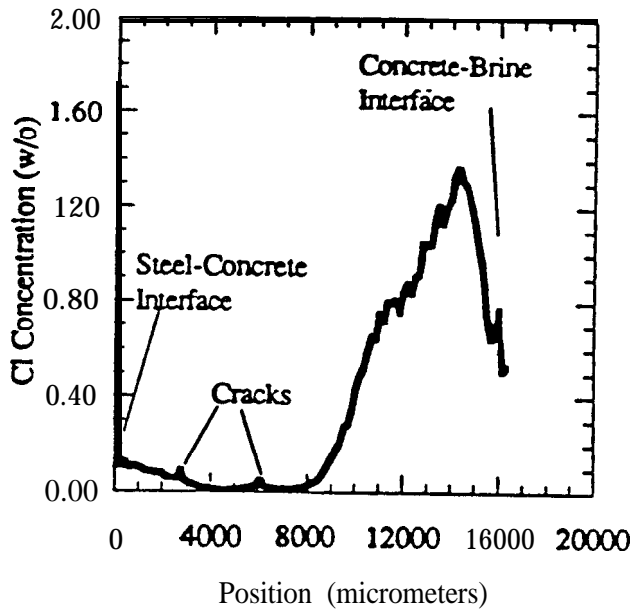


Figure 4a. Cl concentration versus position for the 5% latex modified mortar liner exposed to brine for 60 days.

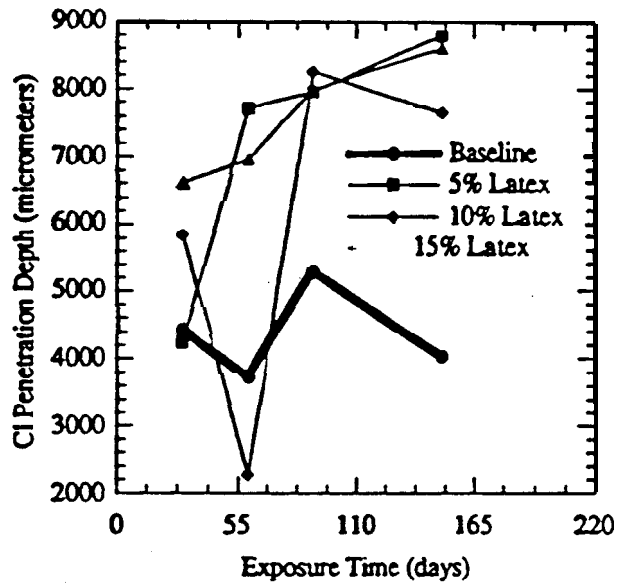


Figure 5. Cl penetration versus exposure time for the baseline and latex modified mortars.

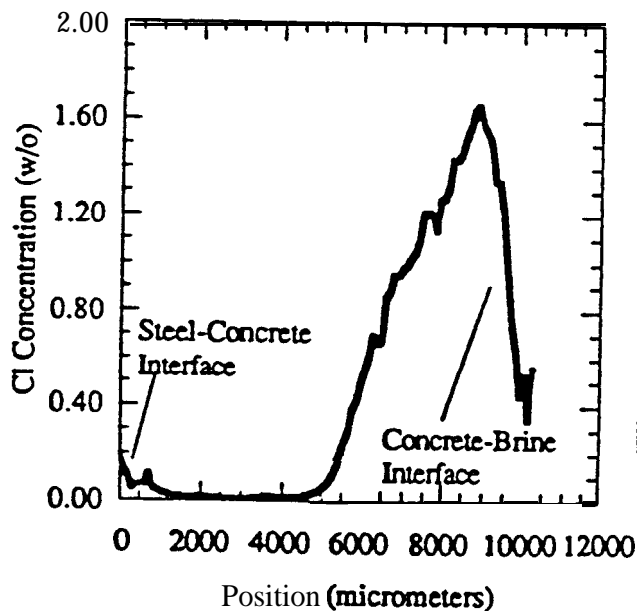


Figure 4b. Cl concentration versus position for the baseline mortar liner exposed to brine for 60 days.

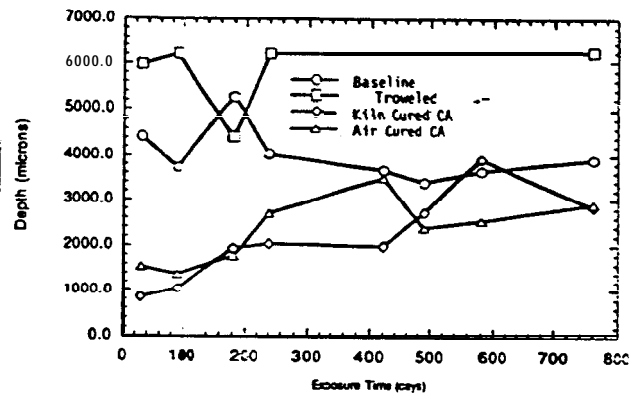


Figure 6a. Cl penetration versus exposure time for the baseline, troweled, and calcium-aluminate mortars.

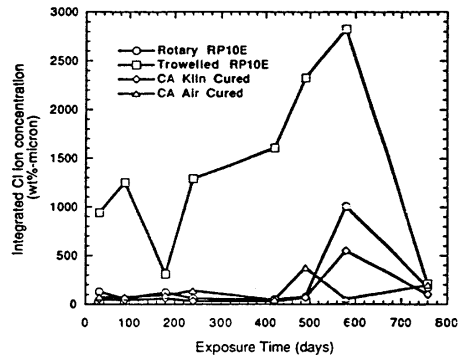


Figure 6b. Cl concentration versus exposure time for the baseline, troweled, and calcium-aluminate mortars.

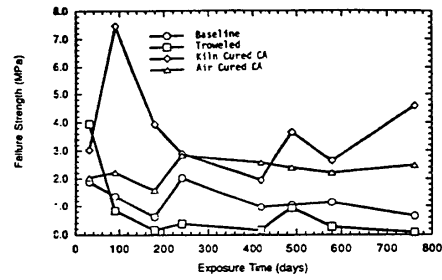


Figure 8. Interfacial shear strength for baseline, troweled, and calcium-aluminate mortars.

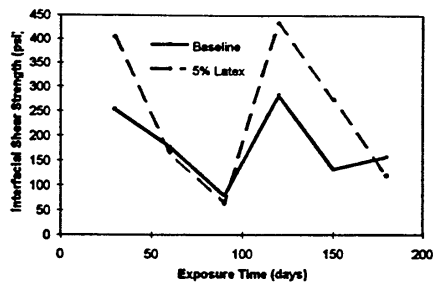


Figure 7. Interfacial shear strength for 5% latex and baseline mortars for exposure times up to 180 days.

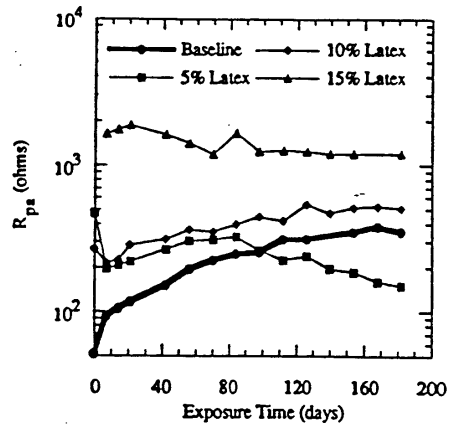


Figure 9. High frequency response. R_{pa}^m versus exposure time for the baseline and latex modified mortars.

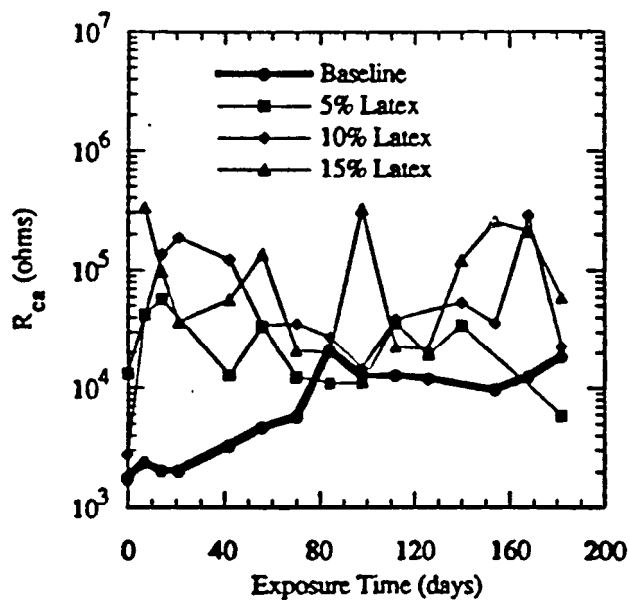


Figure 10. Low frequency response. R_{ca}^m versus exposure time for the baseline and latex modified mortars.

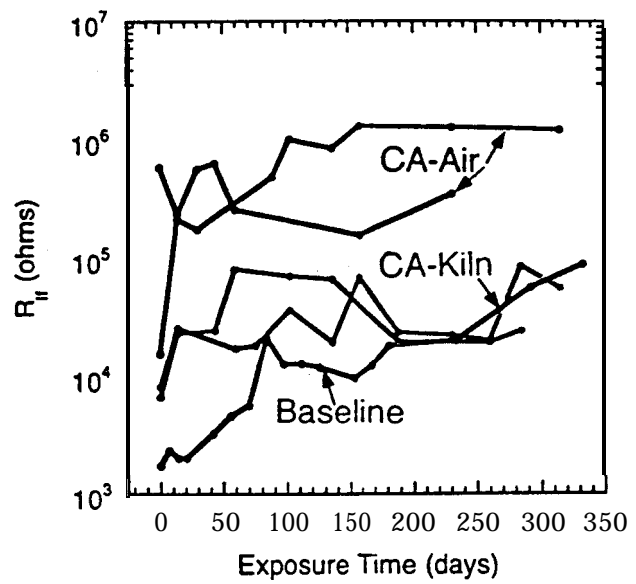


Figure 12. Low frequency response. R_{ca}^m versus exposure time for the baseline, troweled and calcium-aluminate mortars.

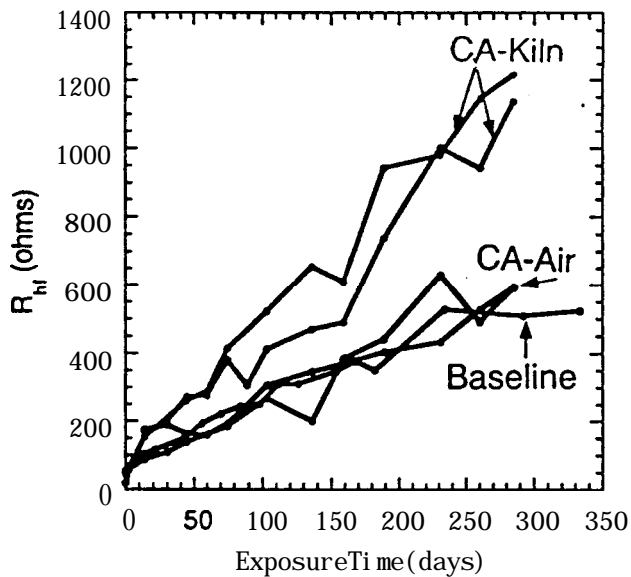


Figure 11. High frequency response. R_{pa}^m versus exposure time for the baseline, troweled and calcium-aluminate mortars.